J Solid State Electrochem (2012) 16:2767–2775
DOI 10.1007/s10008-012-1687-6

ORIGINAL PAPER

Mobility of protons in 12-phosphotungstic acid and its acid and neutral salts

Alexander Igorevich Chikin · Alexander Vladimirovich Chernyak · Zhao Jin · Yulia Sergeevna Naumova · Alexander Evgenevich Ukshe · Nina Vladimirovna Smirnova · Vitaliy Ivanovich Volkov · Yury Anatolevich Dobrovolsky

Received: 19 January 2012 / Revised: 8 February 2012 / Accepted: 11 February 2012 / Published online: 7 March 2012

Abstract The proton mobility in 12-phosphotungstic heteropolyacid (PWA) and its salts ($Cs_2HPW_{12}O_{40}{\cdot}xH_2O$, $Cs_3PW_{12}O_{40}{\cdot}xH_2O$, $(NH_4)_3PW_{12}O_{40}{\cdot}xH_2O$) was investigated by impedance spectroscopy and nuclear magnetic resonance with pulsed field gradient under wide range of relative humidity. Values of two diffusion components observed in PWA as well as in its acid cesium salt differ in one order of magnitude. Also there are two components in the impedance spectra of these compounds. Thus, we suggest, the proton transport take place both inside the grains and along its boundaries. Self-diffusion coefficients, observed in the neutral cesium and ammonium salts, are close to each other and equal to the fast diffusion coefficient in acid cesium salt. At the same time, there is the only relaxation component in the impedance spectra of neutral salts. Thus, it can be concluded, that in case of neutral salts of PWA, there is no proton transport inside the grains of these compounds, and their high proton conductivity caused by fast proton transport along the grain boundaries.

Keywords Heteropoly compound · Proton transport · Impedance spectroscopy · Nuclear magnetic resonance

A. I. Chikin · A. V. Chernyak · Z. Jin · A. E. Ukshe · V. I. Volkov · Y. A. Dobrovolsky (✉)
Institute of Problems of Chemical Physics,
Russian Academy of Science,
Akad. Semenov's Avenue, 1,
Chernogolovka, Moscow Region, Russia 142432
e-mail: dobr62@mail.ru

Y. S. Naumova · N. V. Smirnova
South Russia State Technical University,
Novocherkassk, Russia

Introduction

Heteropoly compounds (HPC) constitute a large group of polybasic acids and their salts. These compounds contain a complex anion named heteropolyanion where heteropolyatom is surrounded by a cage of several oxometallate polyhedrons. There are a lot of different structures of heteropolyanions, but most of them are modifications of three basic types: Keggin structure $[X^{n+}M_{12}O_{40}]^{(8-n)-}$, Dawson structure $[(X^{n+})_2M_{18}O_{62}]^{(16-2n)-}$ and Anderson structure $[X^{n+}M_6O_{24}]^{(8-n)-}$. In these structures, the central atom (X) is typically P or Si; however, over 65 elements are able to act as the complexing heteroatom. M is generally W or Mo with other transition metals such as V, Nb, Ta being less common [1].

HPCs have been studied for more than a century and a half. As a result, a number of applications have been found for HPCs in different areas of science and technology [1, 2]. For example, they are used as effective catalysts in organic synthesis [3], as well as largely employed in analytical chemistry [1]. Unique structure and a large variety of distinctive properties make HPCs attractive targets for both fundamental research and practical applications.

One of the properties, which attracts attention of many researchers to this class of compounds, is the record high proton conductivity in solids (up to 0.18 S cm^{-1} at room temperature for 12-phosphotungstic acid (PWA) discovered in 1979 [4]). Since that a lot of papers have been published on the development of solid electrolytes based on HPCs. Solid proton electrolytes in particular have a good chance to be applied in different electrochemical devices.

High value of proton conductivity is typical not only for heteropoly acids (HPA), but for their salts as well. Most of

these salts can be prepared in the form of water-insoluble powders with high-developed surface, and are furthermore rather thermally stable. Combination of these properties provides a possibility of employment of such compounds both as a proton-conducting component of catalytic materials and doping component of proton exchange membranes for the electrochemical devises, such as fuel cells and gas sensors [5–8]. Moreover it was shown that doping the polymer matrix with HPC resulted not only in high-proton conductivity of such membrane, but in electrocatalytic activity on the electrode/electrolyte interface as well [9].

At the same time, conductivity of HPCs strongly depends on the degree of aquation, and decreases with the increase of temperature and decrease of relative humidity of surrounding atmosphere [10]. Understanding of the mechanism of conductivity could clarify the reasons of this dependence. However, despite a large number of studies on the mobility of protons in HPAs and their salts, no consensus on the mechanism of conductivity has been achieved. Thus, some authors suggest vehicular conduction mechanism in crystallohydrates of PWA [11], whereas the majority of authors hold to "hop-turn" (Grotthuss) mechanism of conductivity. In the paper [12], the conductivity of HPA is considered to be carried out through the Grotthuss mechanism in acidic solution, which contains Keggin anions.

In case of neutral salts of HPAs, which have no protons (considered to be the main charge carriers in HPCs) in their own structure, neither the mechanism of conductivity nor the mechanism of charge carriers generation is still uncertain. In order to explain the presence of charge carriers in neutral salts, several different hypotheses have been proposed. According to some authors [13, 14], this phenomenon can be explained by proposing intracrystalline dynamic dissociation of water molecules due to interaction with weakly charged external oxygen atoms of heteropolyanions. This is the reason of formation of fluctuation mobile proton-charged defect of the hydrogen bonds network.

$$(PW_{12}O_{40})^{3-} + xH_2O \rightleftarrows [(PW_{12}O_{40})(HO)]^{(3+x)-} \ldots xH^+ \quad (1)$$

According to another hypothesis, proton defects formation is possibly caused by the interaction between Keggin anion and molecules of water in the structure [15]:

$$PW_{12}O_{40}{}^{3-} + 7H_2O \rightleftarrows PW_{11}O_{39}{}^{7-} + H_2WO_4 + 4H_3O^+ \quad (2)$$

or

$$-W-O-W-+3H_2O \rightleftarrows 2-W-O^- + 2H_3O^+ \quad (3)$$

Another explanation of the presence of protons in the structure of neutral salts involves acid impurity, captured during the synthesis [16].

Therefore gaining an insight on the mobility of protons in HPAs and their salts is of great importance.

This study was initiated to investigate the mechanism of proton transport in HPCs with different water contents involving two different analytical methods: nuclear magnetic resonance (NMR) and impedance spectroscopy.

Experiment

For this study, we selected 12-phosphotungstic acid ($H_3PW_{12}O_{40}\cdot xH_2O$), its neutral and acid cesium salts ($Cs_3PW_{12}O_{40}\cdot xH_2O$, $Cs_2HPW_{12}O_{40}\cdot xH_2O$), and neutral ammonium salt ($(NH_4)_3PW_{12}O_{40}\cdot xH_2O$).

A commercial HPA (Acros organics, Geel, Belgium) was purified using ether extraction as described in [17]. Salts of HPA were obtained by neutralizing the adequate quantities of the phosphotungstic acid solution (0.01 M) with the appropriate carbonate solution (0.04 M):

$$2H_3PW_{12}O_{40} + 3(Cat^+)_2CO_3 \rightarrow 2(Cat^+)_{3-x}H_xPW_{12}O_{40}\downarrow + 3H_2O + 3CO_2\uparrow, \quad (4)$$

where, $Cat^+ = NH_4^+$, Cs^+.

In the case of the ammonium salt, any ratio of the initial components gives only neutral (fully substituted) salt in the precipitate, while in the case of the cesium salts the number of substituted protons depends on the acid–base ratio in a linear manner. The composition of the acid cesium salt obtained was confirmed by means of X-ray fluorescent analysis (Komita XART; energy range, 1–40 keV) according to the procedure described in [5].

All the synthesized salts are white water-insoluble powders consisting of spherical particles with a complex structure approximately 100–500 nm in diameter. Microphotographs (SEM, Zeiss LEO, Supra 50 VP, accelerating voltage 3–15 kV) of the salts obtained are shown in the Fig. 1a, c.

All the salts were characterized by means of X-ray diffraction analysis (by XRD, Thermo ARL X'TRA, operating with a Cu Kα radiation (λ=1.541 Å) generated at 40 kV and 100 mA with a scan rate of 1° min^{-1} in the angle range of 10–70°) after permanent exposition under phosphorous pentoxide (RH=0%). Specific surface area (S) measurements were held by NOVA 1200e (Quantachrome instruments) after 2 h of degasification at 200 °C.

Water content (xH_2O) was calculated from the mass loss, measured by means of the thermogravimetric analysis (by STA 409 PC Luxx, heat rate 10° min^{-1}) in the temperature range 20–200 °C for all the samples after its exposition at various relative humidities (see Table 1). Also water content of the samples was measured by means of Karl Fischer titration. Accurately weighed samples were placed into

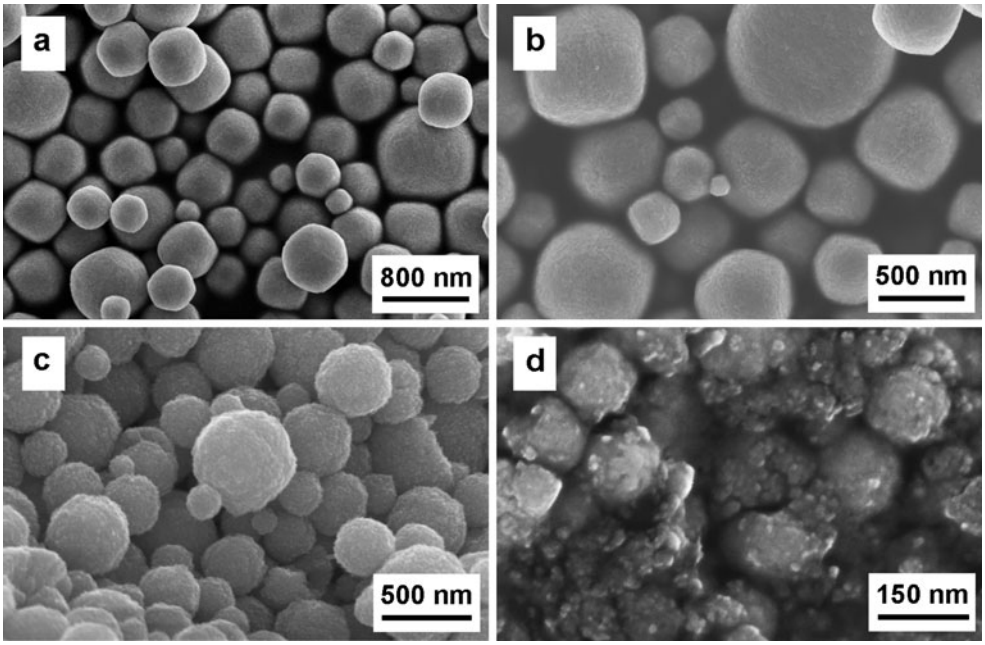

Fig. 1 Microphotographs of salts **a** $(NH_4)_3PW_{12}O_{40}{\cdot}xH_2O$, **b** after heating at 400 °C, **c** $Cs_3PW_{12}O_{40}{\cdot}xH_2O$, **d** after heating at 200 °C

5 ml of dry methanol and stirred for an hour. Automatic zero burette were used for the titration with the Karl Fisher reagent. The titration endpoint was determined visually. Results obtained by two methods, mentioned above, were in a good agreement and were given in Table 1, as well as results of XRD (lattice parameter *a*) and specific surface area measurements.

The average elementary particle size of the salts was found to be 8–10 nm by specific surface area measurements as well as from X-ray diffraction data using Scherrer equation. Moreover, it was discovered, that heating the cesium salt up to 200 °C leads to decomposition of the spherical agglomerates into smaller particles with a characteristic size of 8–10 nm (Fig. 1d). Therefore, a structure model of salt particles has been proposed, according to which, larger spherical 100–500 nm agglomerates consist of close-packed single-crystal particles of 8–10 nm in diameter (Fig. 2).

The ammonium salt has the same microstructure. During the heating even up to the decomposition starting temperature (400 °C), only reversible water loss is observed (Fig. 1b), but larger spherical agglomerates are still stable.

In contrast to the salts, the heteropoly acid has a more simple, nonporous microstructure and consists of discrete crystallites with the size of up to 1 μm. As a result, the HPA has a low specific surface area value.

Proton conductivity measurements were made using the impedance method with impedance meter Elins Z-3000 at the frequency range 0.1 Hz–2 MHz and the amplitude of applied signal of 50 mV. The two-electrode symmetric cells with titanium electrodes were used.

To measure the impedance spectra, HPCs were held under the relative humidity conditions (given in Table 1) till the mass was constant and then compressed under pressure of 2 t cm^{-2} into pellets of 5 mm in diameter and 0.3–4.2 mm thick. Cells were placed into sealed glass vessels with a corresponding relative humidity. The conductivity values were determined from the impedance spectra, recorded at temperature of 25 °C.

NMR investigations were carried out on the samples after their permanent exposition under corresponding relative humidity conditions. The ^{1}H and ^{31}P NMR spectra dependent on humidity were recorded on the high-resolution Bruker

Table 1 Specific surface area, lattice parameter, and water content of HPCs

HPC	*S*, $m^2\ g^{-1}$	*a*, Å	*x*(H_2O)			
			RH=10%	RH=32%	RH=75%	RH=95%
$H_3PW_{12}O_{40}{\cdot}xH_2O$	6	12.140	6	7.5	21	29
$Cs_3PW_{12}O_{40}{\cdot}xH_2O$	102	11.835	6	7.5	10	12
$Cs_2HPW_{12}O_{40}{\cdot}xH_2O$	113	11.820	6	10	10	12
$(NH_4)_3PW_{12}O_{40}{\cdot}xH_2O$	120	11.620	5	9	11	11

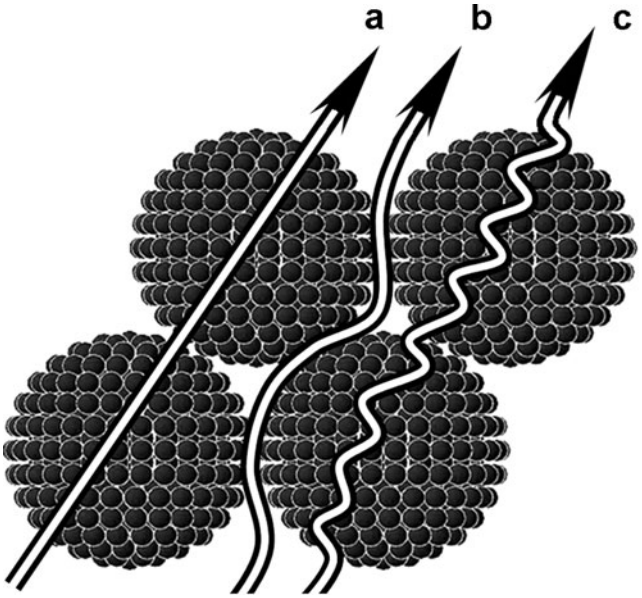

Fig. 2 Schematic model of the proton transport pathway in the structure of HPA salts. **a** Proton transfer inside the grains, **b** on the surface of large agglomerates, and **c** on the surface of small grains into the large agglomerates

AVANCE III 500 spectrometer at room temperature (22–25 °C). NMR frequencies were 500 and 202 MHz for ^{1}H and ^{31}P nuclei, accordingly. The self-diffusion measurements were done by the pulsed field gradient NMR technique using Diff 60 system of the Bruker Avance III 400 solid NMR spectrometer. The signals of ^{1}H spin echo obtained by the stimulated echo sequence depending on pulsed field gradient amplitude were analyzed. The NMR ^{1}H frequency was 400 MHz. The procedure of self-diffusion coefficients measurements in heterogeneous systems is given in detail in [18].

Results and discussion

^{1}H and ^{31}P NMR spectra were obtained for all compounds in the study. ^{31}P spectra are the wide singlet line, the value of chemical shift is varied from 13.2 to 13.9 ppm. The line position does not depend on the sample water content. It is indicated that phosphor surrounding for all structures is the same and sorbed water molecules do not influence the anion structure.

Figure 3 shows the ^{1}H NMR spectra for $H_3PW_{12}O_{40}\cdot xH_2O$, $Cs_2HPW_{12}O_{40}\cdot xH_2O$, $Cs_3PW_{12}O_{40}\cdot xH_2O$, $(NH_4)_3PW_{12}O_{40}\cdot xH_2O$ at different relative humidities.

Overall, ^{1}H NMR spectra of all the compounds in the study consist of a symmetrical broad singlet, shifted downfield relative to the signal of protons of water molecules (4.7 ppm) with the exception of the ammonium salt under low-humidity conditions. This shift is typical for acid aqueous solutions or acidic ion-exchange membranes and it appears because of the existence of hydrated protons, $H^{+}\cdot(H_2O)_x$ [19]. On the spectrum of the ammonium salt (Fig. 3d), there is also a signal of the protons of $(NH_4)^{+}$

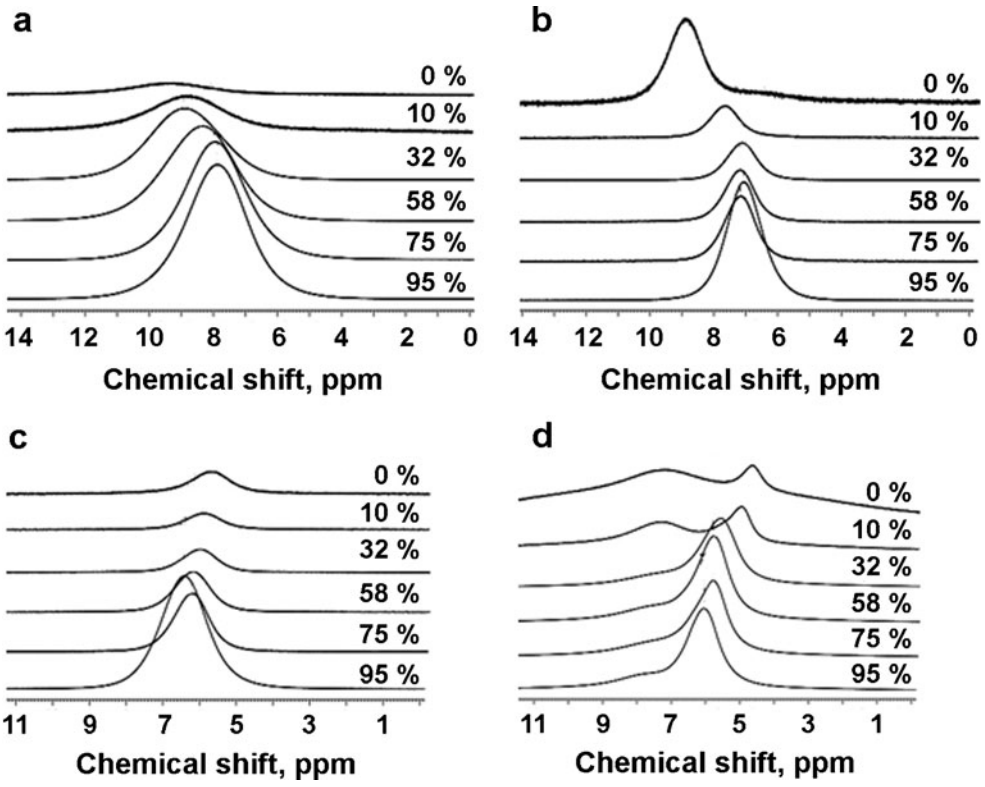

Fig. 3 ^{1}H NMR spectrum of **a** $H_3PW_{12}O_{40}\cdot xH_2O$, **b** $Cs_2HPW_{12}O_{40}\cdot xH_2O$, **c** $Cs_3PW_{12}O_{40}\cdot xH_2O$, **d** $(NH_4)_3PW_{12}O_{40}\cdot xH_2O$ at different relative humidities (values indicated in the figure)

groups (7.3–7.4 ppm), and its position is practically independent of the ambient humidity.

In addition, on the spectra of the neutral salts ($(NH_4)_3PW_{12}O_{40}\cdot xH_2O$, $Cs_3PW_{12}O_{40}\cdot xH_2O$; Fig. 3c, d) upfield shifting of the proton signals of water molecules is observed while humidity decreasing. It is the characteristic effect for the case, when the alkali metal cations are involved into the network formation of hydrogen bonds among the water molecules [19–22]. Heavy cation in the structure causes a weakening of hydrogen bonds and, consequently, reduces the shielding of hydrogen atoms by electrons. While the number of water molecules decreases, the cation influence increases, and the position of the signal progressively shifts to high field end.

Shifting of ^1H NMR signal downfield is observed with the decrease in humidity in the NMR spectra of the acid salt ($Cs_2HPW_{12}O_{40}\cdot xH_2O$) and heteropoly acid ($H_3PW_{12}O_{40}\cdot xH_2O$). Such behavior is typical when the acidic protons of the anion are involved to the organization of hydrogen bonds between the water molecules [19, 20, 23].

Self-diffusion coefficients of protons were measured by NMR with pulsed field gradient for all the compounds in this study. Dependencies of the spin-echo signal intensity on the square of amplitude of the magnetic field gradient (diffusion decay) have a complex shape and can be approximated by the sum of two or three exponential components (Fig. 4).

These components indicate that there are two or three areas (phases) of HPC, with different translational mobility of protons. Therefore, we can define the partial self-diffusion coefficients and the relative proportions of the diffusant in the phases. The procedure for such calculations is described in [18]. Dependencies of the partial self-diffusion coefficients on relative humidity are shown in Fig. 5.

For the HPA, diffusion decay is characterized by the sum of two exponents. Thus there are two types of protons with different transitional mobility and corresponding values of partial self-diffusion coefficients ($D\sim10^{-12}$ and 10^{-13} m^2 s^{-1}) under low-humidity conditions (1 and 2 of Fig. 5). While humidity increases these values grow symbatically and increase rapidly to the value of $D\sim10^{-10}$ m^2 s^{-1} at a relative humidity close to 95%.

The slow diffusion component ($D\sim10^{-12}$ m^2 s^{-1}; 5 of Fig. 5) has also been found in the acid cesium salt. But in spite of slow protons there are two kinds of protons with high mobility with the corresponding values of self-diffusion coefficient near to $D\sim10^{-10}$ m^2 s^{-1} in the structure of $Cs_2HPW_{12}O_{40}\cdot xH_2O$ (4 and 5 of Fig. 5). In the case of neutral ammonium and cesium salts, only two fast diffusion components have been found ($D\sim10^{-10}$ m^2 s^{-1}), which were close to each other (6–9 of Fig. 5).

Proton conductivity of samples has been measured by the method of impedance spectroscopy. The parameters of equivalent scheme were determined from experimental spectra after compensating the geometrical capacity and line inductance of the measuring cell by the fitting procedure. The equivalent circuit contains the electrode impedance and the elements, representing the volume relaxation (Fig. 6). In order to check the attribution of the components to the volume impedance, the measurements have been taken with different thicknesses of the tablets.

The typical impedance spectrum of the cell with phosphotungstic acid (also typical for the acid cesium salt of HPA) is shown in Fig. 6a. For the acid and the acid cesium salt, the volume relaxation contains two components,

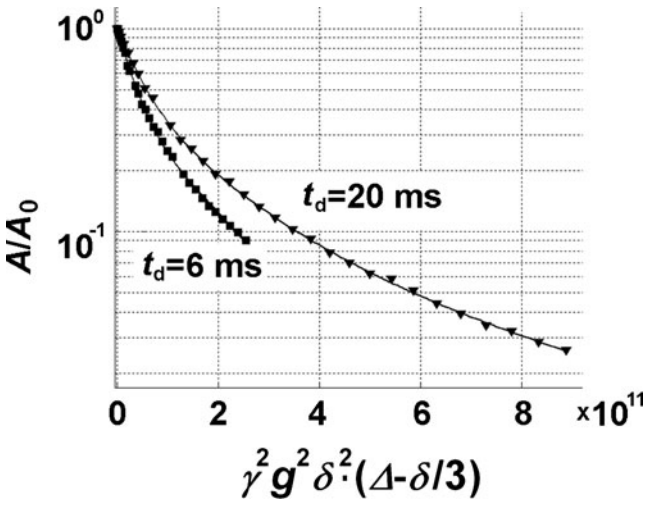

Fig. 4 Diffusion decay of spin-echo signal of ^1H in $H_3PW_{12}O_{40}\cdot21H_2O$ with different diffusion time t_d=6 ms (D_s=6.3·10^{-12} m^2 s^{-1}, D_f=3.4·10^{-11} m^2 s^{-1}) and t_d=20 ms (D_s=1.3·10^{-12} m^2 s^{-1}, D_f=1.5·10^{-11} m^2 s^{-1})

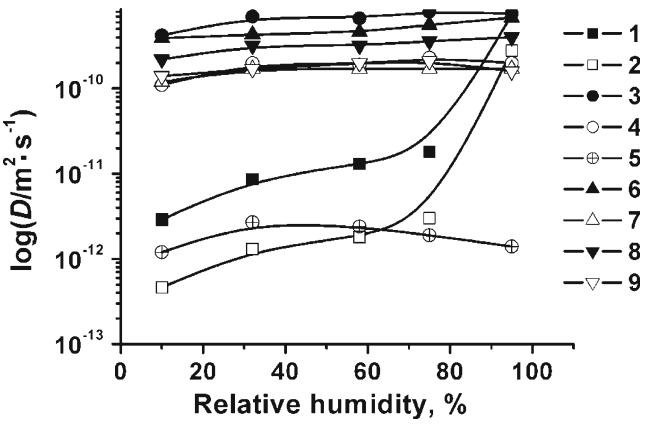

Fig. 5 Dependence of the self-diffusion coefficients on relative humidity. *1–2* $H_3PW_{12}O_{40}\cdot xH_2O$, *3–5* $Cs_2HPW_{12}O_{40}\cdot xH_2O$, *6–7* $Cs_3PW_{12}O_{40}\cdot xH_2O$, *8–9* $(NH_4)_3PW_{12}O_{40}\cdot xH_2O$. *Filled symbol* fast diffusion, *empty symbol* slow diffusion

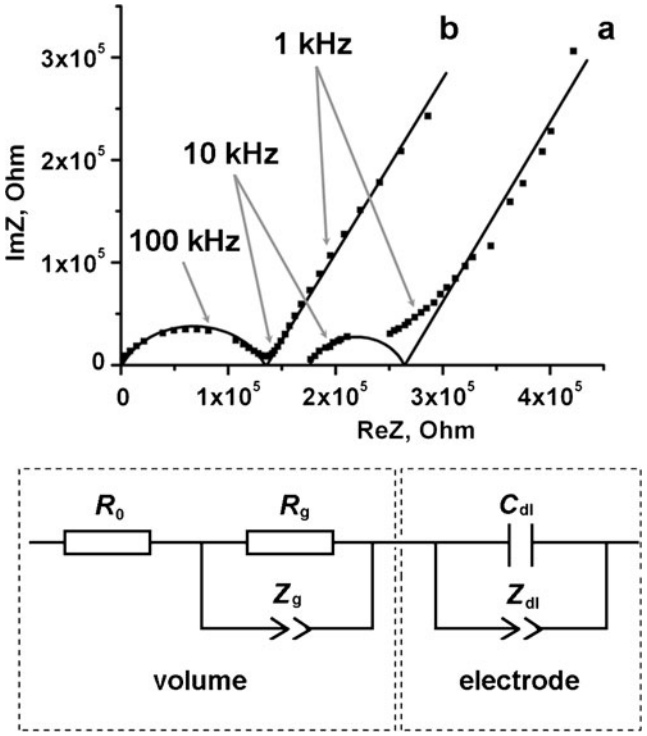

Fig. 6 Impedance hodograph of HPA (**a**) (also typical for its acid cesium salt) and neutral ammonium salt (**b**) (also typical for neutral cesium salt) at RH=0% and the corresponding equivalent circuit

indicating two spatially separated mechanisms of conduction, which can be attributed to the processes of proton transport inside the grains and at their surface.

Thus, the impedance spectra of the cells with the HPA and the acid cesium salt can be described by an equivalent circuit (Fig. 6). Elements R_0 and $R_g||Z_g$ refer to the volume relaxation, which is confirmed by the proportional dependence of R_0 and R_g on the thickness of the samples; $C_{dl}||Z_{dl}$ is an electrode effect (the relaxation of double electric layer). It can be assumed that the R_0 describes the proton transport inside the grains, and the R_g corresponds to the proton transfer trough the surface of grains.

For the neutral ammonium and cesium salts (Fig. 6b), the relaxation process of the volume part of impedance was observed only. It means that one of the proton transport pathways has disappeared. Namely, according to our hypothesis, the link R_0 completely drops out from the above equivalent circuit, so the proton transport inside the grains is blocked.

Thus, according to NMR with pulsed-field gradient and impedance spectroscopy, there are two types of hydrated protons with different mobility in compounds with acidic protons in the structure ($H_3PW_{12}O_{40}{\cdot}xH_2O$, $Cs_2HPW_{12}O_{40}{\cdot}xH_2O$), while in the neutral salts, translational mobility of hydrated complexes is characterized by only one self-diffusion coefficient.

Relationship between the values of self-diffusion coefficients and conductivity can be obtained from the Nernst-Einstein equation and is known to be expressed as follows:

$$\sigma = ne^2 \frac{D}{kT} \tag{5}$$

where, n is a number of charge carriers per unit volume, $e=1.9\times10^{-19}$ (C) is an electron charge, D is a self-diffusion coefficient ($m^2\ s^{-1}$), $k=1.38\times10^{-23}$ ($J\ K^{-1}$)—Boltzmann constant, $T=293$ (K)—temperature.

Ionic conductivities of HPA, calculated by Eq. 5 are lower than the ones obtained from impedance spectra (Table 2). The partial diffusion coefficients decrease with increasing the diffusion time (t_d): $t_d=\Delta-\delta/3$ (where Δ is interval between gradient pulses, δ is gradient pulse duration; Fig. 6a). The population density of slow diffusion component falls down with diffusion time by exponential law. It means that there are space limitations for diffusion. So we can calculate a size of diffusion way for each component according to [24, 25]. The decreasing of the partial self-diffusion components with increasing of diffusion time (Fig. 7a) gives the size of diffusion way for the slow component (r_s) as $r_s\leq100$ nm and for the fast component $r_f\geq500$ nm. So it is possible that the slow component is terminated by grain size. The decrease of the slow-component population with increase of diffusion time (Fig. 7b) allowed us to calculate the exchange time for protons of slow and fast phases which is about 7 ms,

Table 2 Comparison of the HPA conductivities, determined by the impedance spectroscopy and obtained from self-diffusion coefficients

Relative humidity, %	10	32	58	75	95
$x(H_2O)$	6	7.5	12	20	29
D_f, $m^2\ s^{-1}$	$2.9\cdot10^{-12}$	$8.6\cdot10^{-12}$	$1.3\cdot10^{-11}$	$2.1\cdot10^{-11}$	$7.3\cdot10^{-10}$
D_s, $m^2\ s^{-1}$	$4.6\cdot10^{-13}$	$1.3\cdot10^{-12}$	$1.8\cdot10^{-12}$	$1.8\cdot10^{-12}$	$2.8\cdot10^{-10}$
σ_{Df}, $S\ cm^{-1}$, calc from D_f	$7.9\cdot10^{-4}$	$2.3\cdot10^{-3}$	$3.4\cdot10^{-3}$	$5.3\cdot10^{-3}$	$1.1\cdot10^{-1}$
σ_{Ds}, $S\ cm^{-1}$, calc from D_s	$1.3\cdot10^{-4}$	$0.35\cdot10^{-3}$	$0.34\cdot10^{-3}$	$0.9\cdot10^{-3}$	$0.42\cdot10^{-1}$
σ_f, $S\ cm^{-1}$ calc by (7)	$8.3\cdot10^{-4}$	$2.0\cdot10^{-3}$	$6.4\cdot10^{-3}$	$13.0\cdot10^{-3}$	$1.96\cdot10^{-1}$
σ_s, $S\ cm^{-1}$ calc by (6)	$5.2\cdot10^{-4}$	$1.3\cdot10^{-3}$	$4.0\cdot10^{-3}$	$10.0\cdot10^{-3}$	$1.5\cdot10^{-1}$
σ_f/σ_{Df}	1	1	2	2	2
σ_s/σ_{Ds}	4	3.5	10	10	3.6

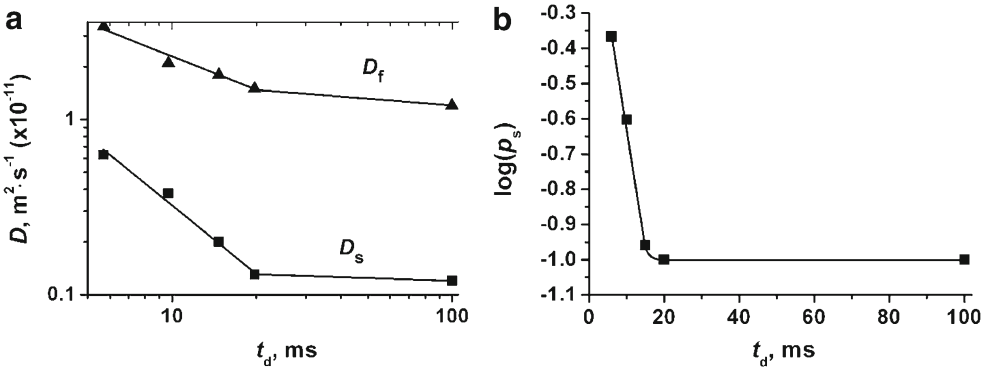

Fig. 7 Dependencies of fast (D_f) and slow (D_s) self-diffusion coefficients (**a**) and of the relative weigh of the slow component on diffusion time (**b**), the decreasing of the apparent population is caused by spin-lattice relaxation in the range of diffusion time from 20 to 100 ms, T_1=300 ms in $H_3PW_{12}O_{40}{\cdot}21H_2O$

corresponding to frequency region 100–150 Hz. Therefore, the "slow" diffusion of protons D_s in HPA, in our assumption, apparently corresponds to the proton transport inside one HPA grain. However by impedance measurement, the conductivity of the HPA grain has to be equal:

$$\sigma_s = \frac{L}{\pi \times r^2} \times \frac{1}{R_0 + R_g} \tag{6}$$

where, L is a thickness of the pellet and r is its radius.

The fast diffusion may be related to the proton transport along the surface of grains (R_g). It also should be taken into account that the path of proton transport is at least $\pi/2$ times longer than the transport distance directly through the grains (as it is schematically shown in Fig. 2); thus, the complex resistance should be $\pi/2$ times higher. That means the macroscopic conductivity (corresponding to this transport) can be calculated with the following formula:

$$\sigma_f = \frac{L}{\pi \times r^2} \times \frac{1}{R_g \times \frac{\pi}{2}} \tag{7}$$

It is assumed that all three protons of HPA are involved in the proton transfer process (n=3). The values of diffusion coefficient (D_f and D_s) and conductivity (σ_{Df} and σ_{Ds}), calculated using Nernst–Einstein Eq. 5 are shown in Table 2. Moreover, the values of conductivity (σ_f and σ_s), obtained from impedance spectroscopy and calculated using the formulas (6) and (7) are also sown in this table.

For the "fast" diffusion transport parameters of proton, determined by the nuclear magnetic resonance with pulsed field gradient (PFG-NMR) and defined from the conductivity are equal in the case of small water contents. In the same conditions, transport parameters of proton, obtained using the methods mentioned above, differs only slightly (three to four times) for the slow diffusion (Fig. 8). However, when the value of water contents achieves about 10 molecules per HPA molecule, the situation changes dramatically. The "fast" transport according to the PFG-NMR becomes twice slower than that determined from the conductivity. This difference is due to the big increase of the mobility, determined by the relaxation impedance spectra. The discrepancy in the "slow" transport is even bigger, and reaches one order of magnitude, decreasing only at 95% humidity, close to dissolving boundary (see Table 2).

In order to explain the observed effects, the following hypothesis can be suggested. It is known that the increased proton conductivity is observed because of the water film on the solid surface with highly polarized oxygen atoms [26–28]. The additional conductivity appears due to the presence of excess ions on the surface (the ions of the electrical double layer). So, the conductivity of a quasi-liquid layer on

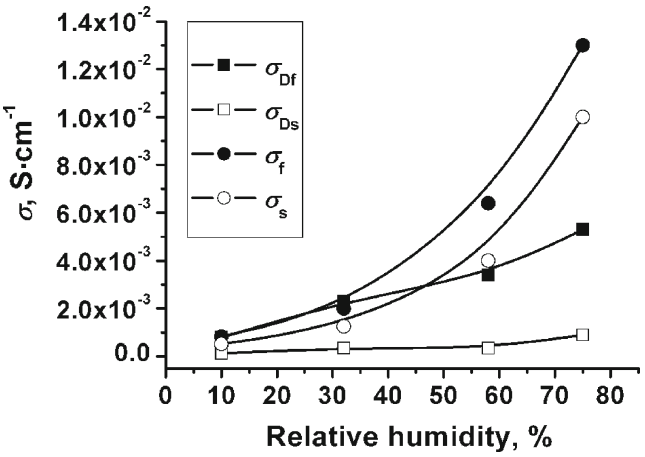

Fig. 8 Dependence of the conductivity of HPA, calculated by impedance and self-diffusion coefficients on the values of relative humidity (in the range from 0% to 75% RH)

Table 3 Calculated charge carriers amounts in the neutral salts of HPA

Relative humidity,%	n, unit per molecule	
	$(NH_4)_3PW_{12}O_{40}{\cdot}xH_2O$	$Cs_3PW_{12}O_{40}{\cdot}xH_2O$
10	$4{\cdot}10^{-2}$	$3{\cdot}10^{-3}$
32	$3{\cdot}10^{-2}$	$6{\cdot}10^{-3}$
58	$4{\cdot}10^{-2}$	$7{\cdot}10^{-4}$
75	$6{\cdot}10^{-2}$	$2{\cdot}10^{-4}$
95	$8{\cdot}10^{-2}$	$3{\cdot}10^{-5}$

the ice surface is three orders of magnitude higher than of the pure water [28]. A similar effect should also be observed on the surface of crystalline hydrate with ice-like water structure, and in particular on the surface of HPA crystallites.

Also, the discrepancy in the calculated values of ionic conductivity can be explained by the fact that at high moisture content, while forming a continuous network of hydrogen bonds, the main contribution to charge transfer process provides the Grotthuss mechanism, not vehicular. However, self-diffusion measured by NMR is determined by the translational transfer of proton spin and it does not include the charge transfer by Grotthuss mechanism.

In the structure of the acid cesium salt, the protons with low mobility which move within the grain have also been found. However, in contrast to HPA, in its salts possessing a complex microstructure (including the acid cesium salt) significant increase of proton mobility is observed assuming self-diffusion coefficients obtained. The outstanding feature of HPA salts in the study is their high-developed surface due to the complex microstructure of their particles. Therefore, the high proton mobility might be based on the Grotthuss transport though the surface water molecules, in other words through the grain boundaries.

There are three possible proton transport pathways in such complex structures (Fig. 2). "*A*" denotes the transport of protons inside "elementary" grains. For the HPA salts, the high proton mobility is observed on the paths *b* and *c* (on the surface of the large agglomerates and on the boundaries of small particles). Self-diffusion coefficients of these processes have similar values, so proton transfer processes *b* and *c* do not differ in the impedance spectroscopy, but they can be discerned by NMR.

In neutral salts, bulk conductivity (inside small grains, pathway *a*) is extremely low, and charged particles transport is carried out along the *b* and *c* pathways. This conduction mechanism of neutral salts is well confirmed by impedance spectroscopy and by the obtained self-diffusion coefficients. High values of conductivity of these compounds are apparently provided with a high mobility of charge carriers, while their quantity is very small. Quantities of charge carriers in the neutral ammonium and cesium salts at different values of humidity, calculated by the Nernst–Einstein equation, are shown in Table 3.

It is known [29] that the water, located in nanopores, has a structure distinct from that of free water. The interaction of water molecules with the charged pore walls leads to changes in direction, average number and strength of the hydrogen bonds. Reducing the number of hydrogen bonds increases the mobility of protons with the Grotthuss mechanism. It seems this behavior is typical for water in the pores of the complex structure of insoluble HPC, which makes it a possible reason of high mobility of charge carriers on the grain boundary of such structure.

Conclusions

The nature of proton transport in the structures of phosphotungstic heterpoly acid and its salts was investigated by the NMR relaxation of protons and impedance spectroscopy. It was found that proton conductivity of phosphotungstic acid has two (volumetric and superficial) components. Proton transport of the insoluble acid salts of HPA is also possible in the bulk and trough the crystallites surface as well. On the one hand, there are fewer charge carriers in acid salt than in HPA; from the other hand, its complex structure provides a highly developed system of surface-absorbed water, so the transport through the surface water makes the main contribution to the proton conductivity mechanism.

As for the neutral salts of HPA, the large value of the conductivity is fully provided by the high proton mobility along the grain boundaries inside the spherical agglomerates and at its surface. The proton transport inside the crystallites of neutral salts is absent or greatly hindered.

References

1. Nikitina EA (1962) Geteropolisoedineniya (Hetropoly compounds). Goskhimizdat, Moscow
2. Mioc UB, Todorovic MR, Davidovic M, Colomban Ph, Holclajtner-Antunovic I (2005) Solid State Ionics 176:3005–3017
3. Okuhara T, Mizuno N, Misono M (2001) Appl Catal A 222:63–77
4. Nakamura O, Kodama T, Ogino I, Miyake Y (1979) Chem Lett 1:17–18
5. Chzhao T, Ukshe AE, Leonova LS, Dobrovol'skii YA (2011) Russ J Electrochem 47:595–604
6. Antolini E, Gonzalez ER (2010) Appl Catal, B 96:245–266
7. Korotcenkov G, Han SD, Stetter JR (2009) Chem Rev 109:1402–1433
8. Dupuis AC (2011) Prog Mater Sci 56:289–327
9. Treglazov I, Leonova L, Dobrovolsky Yu, Ryabov A, Vakulenko A, Vassiliev S (2005) Sens Actuators B 106:164–169
10. Korosteleva AI, Leonova LS, Ukshe EA (1987) Sov Electrochem 23:1266–1270
11. Kreuer KD, Hampele M, Dolde K, Rabenau A (1988) Solid State Ionics 28–30:589–593
12. Yaroslavtsev AB (1994) Russ Chem Rew 63:429–435
13. Ukshe EA, Leonova LS, Korosteleva AI (1989) Solid State Ionics 36:219–223
14. Matachowski L, Zieba A, Zembala M, Drelinkiewicz A (2009) Catal Lett 133:49–62
15. Yaroslavtsev AB, Yaroslavtseva EM, Chuvaev VF (1990) J Inorg Chem USSR 35:2769–2775
16. Holclajtner-Antunovic I, Mioc UB, Todorovic M, Janovic Z, Davidovic M, Bajuk-Bogdanovic D, Lausevic Z (2010) Mater Res Bull 45:1679–1684
17. Matijevic E, Kerker M (1959) J Am Chem Soc 81:1307
18. Volkov VI, Korotchkova SA, Ohya H, Guo Q (1995) J Membr Sci 100:273–286
19. Creekmore RW, Reilley CN (1970) Anal Chem 42:570–575
20. Volkov VI, Sidorenkova EA, Timashev SF, Lakeev SG (1993) Russ J Phys Chem 67:914–918
21. Volkov VI, Volkov EV, Timofeev SF, Sanginov EA, Pavlov AA, Safronova EY, Stenina IA, Yaroslavtsev AB (2010) Russ J Inorg Chem 55:318–324

22. Saldadze GK, Tagirova RI, Volkov VI (1993) Russ J Phys Chem 67:1818–1824
23. Volkov VI, Saldadze GK, Tagirova RI, Kropotov LV, Khustishivi VG, Shaprtko NN (1989) J Phys Chem 63:1005–1011
24. Suh KJ, Hong YS, Skirda VD, Volkov VI (2003) Biophys Chem 104:121–130
25. Cho JH, Hong YS, Skirda VD, Volkov VI (2003) Magn Reson Imaging 21:1009–1017
26. Kumar N, Kent PRC, Bandura AV, Kubicki J, Wesolowski DJ, Cole DR, Sofo JO (2011) J Chem Phys 134:044706
27. Zyubina TS, Dobrovolskii YA (1995) Russ J Electrochem 31:1280–1284
28. Skinner B, Loth MS, Shklovksii BI (2009) Phys Rew E Stat Nonlinear Soft Matter Phys 80:041925
29. Tejedor-Tejedor MI, Vichi FM, Anderson MA (2005) J Porous Mater 12:201–214